Available online at www.sciencedirect.com
SCIENCE DIRECT®
Journal of Solid State Chemistry 179 (2006) 370–377
JOURNAL OF SOLID STATE CHEMISTRY
www.elsevier.com/locate/jssc

Multianvil high-pressure/high-temperature synthesis, crystal structure, and thermal behaviour of the rare-earth borogermanate $Ce_6(BO_4)_2Ge_9O_{22}$

Gunter Heymann, Hubert Huppertz*

Department Chemie und Biochemie, Ludwig-Maximilians-Universität München, Butenandtstrasse 5-13, 81377 München, Germany

Received 19 September 2005; received in revised form 19 October 2005; accepted 20 October 2005
Available online 6 December 2005

Abstract

The new monoclinic cerium borogermanate $Ce_6(BO_4)_2Ge_9O_{22}$ was synthesized under high-pressure and high-temperature conditions in a Walker-type multianvil apparatus at 10.5 GPa and 1200 °C. $Ce_6(BO_4)_2Ge_9O_{22}$ crystallizes with two formula units in the space group $P2_1/n$ with lattice parameters $a = 877.0(2)$, $b = 1079.4(2)$, $c = 1079.1(2)$ pm, and $\beta = 95.94(3)°$. As the parameter pressure favours the formation of compounds with cations possessing high coordination numbers, it was possible to produce simultaneously BO_4-tetrahedra and GeO_6-octahedra in one and the same borogermanate for the first time. Furthermore, the cerium atoms show high coordination numbers (C.N.: 9 and 11), and one oxygen site bridges one boron and two germanium atoms ($O^{[3]}$), which is observed here for the first time. Besides a structural discussion, temperature-dependent X-ray powder diffraction data are presented, demonstrating the metastable character of this high-pressure phase.

Keywords: High-pressure; Multianvil; Borate; Germanate; Borogermanate; Crystal structure

1. Introduction

Using high-pressure/high-temperature conditions in the synthesis of borates can lead to new metastable but tangible borates with new compositions and special structural motifs. Next to new high-pressure polymorphs like χ-$RE$$BO_3$ (RE = Dy–Er) [1] or new *meta*-borates such as β-$RE(BO_2)_3$ (RE = Tb–Lu) [2,3] and γ-$RE(BO_2)_3$ (RE = La–Nd) [4,5], it was also possible to synthesize new compositions as $RE_4B_6O_{15}$ (RE = Dy, Ho) [6–8] or α-$RE_2B_4O_9$ (RE = Sm–Ho) [9–11], exhibiting the new structural motif of edge-sharing BO_4-tetrahedra. With the synthesis of $RE_3B_5O_{12}$ (RE = Tm–Lu), we were able to make a silicate-analogous structure by use of high pressure, in which all tetrahedral positions, formerly occupied by Si/Be (semenovite), for the first time were completely substituted by boron (homeotype structure to semenovite) [12].

Recently, we extended our syntheses under high-pressure conditions into the field of rare-earth borogermanates. Interestingly, three-component systems from rare-earth oxides and two acid oxides like boron oxide and germanium oxide never form many ternary systems. Screening the literature, we found that the system RE_2O_3, B_2O_3, and GeO_2 shows only two families of compounds: $RE_{14}(GeO_4)_2(BO_3)_6O_8$ (RE = Pr, Nd, Sm–Gd) [13–19] (earlier designated as $RE_{14}(GeO_4)_2(BO_3)_8O_5$ [13,14]) and $RE$$BGeO_5$. Single crystals of the first family were obtained by spontaneous crystallization from a flux, e.g. $6Gd_2O_3$, $3B_2O_3$, $6GeO_2$, and 85PbO in the case of $Gd_{14}(GeO_4)_2(BO_3)_6O_8$ [18]. Inside the isotypic compounds $RE_{14}(GeO_4)_2(BO_3)_6O_8$, the rare-earth cations exhibit coordination numbers ranging from 6 to 10, which restricts the composition to the rare-earth cations Pr, Nd, and Sm–Gd. The attempts to synthesize analogous compounds with larger and smaller rare-earth cations were unsuccessful. Experiments with terbium oxide resulted in binary borates and germanates [17]. Furthermore, rare-earth ions of different sizes were added to the composition, and in some

*Corresponding author. Fax: +49 89 2180 77806.
E-mail address: huh@cup.uni–muenchen.de (H. Huppertz).

0022-4596/$ - see front matter © 2005 Elsevier Inc. All rights reserved.
doi:10.1016/j.jssc.2005.10.028

cases solid solutions were obtained, which melt congruently. Following that way, the region of existence of this structure type was extended to mixtures of two, three, or four rare-earth's, e.g. $La_7RE_7(GeO_4)_2(BO_3)_6O_8$ (RE = Tb, Dy, Ho, Er) [20,21], $Nd_xSm_yEu_{4-x-y}(GeO_4)_2(BO_3)_6O_8$ [22], and $Nd_xSm_yEu_zGd_{4-x-y-z}(GeO_4)_2(BO_3)_6O_8$ [23]. The solid solution with lanthanum and terbium ($La_xTb_{14-x}(GeO_4)_2(BO_3)_6O_8$) is of special interest, whereas the individual compounds $RE_{14}(GeO_4)_2(BO_3)_6O_8$ with RE = La and Tb are still unknown.

The second family, represented by the formula REBGeO$_5$ [24–29], exhibits two types of structures. For the larger rare-earth ions (RE = La, Pr, and Nd (low-temperature phase)) a trigonal cell symmetry was realized (space group $P3_1$), crystallizing with the REBSiO$_5$ stillwellite structure type (CeBSiO$_5$) [30–33]. Both atoms, germanium and boron, are coordinated tetrahedrally forming helical chains along the c-axes. The smaller rare-earth's (RE = Nd (high-temperature)–Er) were described in a monoclinic cell ($P2_1/a$), isotypic with the datolite-type structure (CaBSiO$_4$OH) [34]. This structure is layered, and the cations are separated by BO$_4$- and GeO$_4$-tetrahedra. For the smallest ions (RE = Tm, Yb, Lu), the compound does not exist until now. Additionally, solid solutions in the system $La_{1-x}Nd_xBGeO_5$ have been investigated. For $0 \leqslant x \leqslant 0.6$ the stillwellite structure was stabilized, and for $x \geqslant 0.8$ the monoclinic modification is observed [28].

Recently, it was shown that boron can be incorporated into germanate frameworks [35–40]. In this context, the combination of borate and germanate groups in the same crystalline material generated a new class of materials with novel framework topologies.

Concerning the structures, all former-mentioned borogermanates are characterized by the combination of trigonal BO$_3$-groups with GeO$_4$-tetrahedra and the combination of BO$_4$-tetrahedra with GeO$_4$-tetrahedra. A third variety of building blocks can be found in the class of transition-metal borogermanates, namely $Ni_5GeB_2O_{10}$ (space group $Pbam$), where the combination of BO$_3$-groups with GeO$_6$-octahedra exists [41]. Missing motives in this series are the combination of BO$_4$-tetrahedra with GeO$_5$-polyhedra or GeO$_6$-octahedra, because germanium may adopt three different coordinations, e.g. four, five, and six [42]. High-pressure conditions should prefer combinations, in which boron and germanium exhibit their highest coordination numbers four and six, respectively. This assumption was confirmed by the borogermanate $Ce_6(BO_4)_2Ge_9O_{22}$, synthesized under conditions of 10.5 GPa at 1200 °C. Afterwards, we describe the synthesis, the structure, and the thermal properties of the new borogermanate $Ce_6(BO_4)_2Ge_9O_{22}$.

2. Experimental part

According to Eq. (1), the compound $Ce_6(BO_4)_2Ge_9O_{22}$ was synthesized via a high-temperature/high-pressure route, using molar mixtures of CeO$_2$ (purity > 99.9%), GeO$_2$ (trigonal, α-quartz type, purity > 99.999%, Chempur, Karlsruhe), and B$_2$O$_3$ (purity > 99.9%, Strem Chemicals, Newburyport, USA).

$$6CeO_2 + 9GeO_2 + B_2O_3 \xrightarrow[1200\,^\circ C]{10.5\,GPa} Ce_6(BO_4)_2Ge_9O_{22} + 3/2O_2. \quad (1)$$

A boron nitride crucible of a 14/8-assembly was loaded with a carefully milled mixture of the compounds, compressed within 3 h to 10.5 GPa, using a multianvil apparatus, and heated up to 1200 °C in the following 10 min. Details of the construction of the assembly can be found in Refs. [43–46]. After a period of 10 min with a constant temperature of 1200 °C, the assembly was cooled down slowly to 700 °C followed by quenching to room temperature. Decompression past, the recovered experimental octahedron was broken apart, and the sample carefully separated from the surrounding hexagonal boron nitride. This procedure led to a slightly yellow to colourless, crystalline composite, consisting of the new borogermanate $Ce_6(BO_4)_2Ge_9O_{22}$, the orthorhombic *meta*-borate γ-Ce(BO$_2$)$_3$ [5], and rests of GeO$_2$ (a *rutile*-type (*argutite*)), which were identified by X-ray powder diffraction.

For an optimization of the synthetic parameters, the synthesis pressure was decreased to 8.5 GPa resulting in a nearly complete prevention of the byproduct γ-Ce(BO$_2$)$_3$ [5]. But, we detected a new phase next to the main phase $Ce_6(BO_4)_2Ge_9O_{22}$ in the powder pattern of this system, unknown until now. Hitherto, it was not possible to obtain a single-phase product by varying the temperature and pressure conditions. An examination of the crystallinity of the sample for the selection of single crystals revealed inadequate quality. Therefore, the experiments were repeated with the addition of a PbO/PbO$_2$-flux (CeO$_2$:GeO$_2$:B$_2$O$_3$:PbO:PbO$_2$ = 6:9:1:12:0.3) at 10.5 GPa and 1200 °C to improve the growth and quality of the crystals to an acceptable size similar to the crystallization of $RE_{14}(GeO_4)_2(BO_3)_6O_8$ (RE = Pr, Nd, Sm–Gd) [13–19]. Single crystals of $Ce_6(BO_4)_2Ge_9O_{22}$ were isolated from the mentioned flux synthesis. The composition and the absence of lead inside the single crystals were checked by EDX analysis. The analysis of the cerium and germanium content in $Ce_6(BO_4)_2Ge_9O_{22}$ via EDX was determined to 12.0 and 17.1 atom%, respectively (theoretical:/atom%: 12.8% Ce, 19.1% Ge).

3. Crystal structure analysis

Small single crystals of $Ce_6(BO_4)_2Ge_9O_{22}$ were isolated by mechanical fragmentation, and examined by Buerger precession photographs. Single-crystal intensity data were collected at room temperature from a regularly shaped colourless crystal (block) by use of a Stoe IPDS detector diffractometer [Mo-$K\alpha$ radiation (71.073 pm)]. A numerical based absorption correction (Habitus [47]) was applied to the intensity data. All relevant information concerning the data collection is listed in Table 1. According to the

Table 1
Crystal data and structure refinement for $Ce_6(BO_4)_2Ge_9O_{22}$

Empirical formula	$Ce_6(BO_4)_2Ge_9O_{22}$
Molar mass ($g\,mol^{-1}$)	1995.65
Crystal system	Monoclinic
Space group	$P2_1/n$ (No. 14)
Single crystal diffractometer	STOE-IPDS
Radiation	Mo-$K\alpha$ ($\lambda = 71.073$ pm)
Single crystal data	
a (pm)	877.0(2)
b (pm)	1079.4(2)
c (pm)	1079.1(2)
β (deg.)	95.94(3)
Volume ($Å^3$)	1016.0(4)
Formula units per cell	$Z = 2$
Temperature (K)	293(2)
Calculated density ($g\,cm^{-3}$)	6.523
Crystal size (mm^3)	$0.03 \times 0.03 \times 0.03$
Detector distance (mm)	50.0
Irradiation/exposure (min)	10
Number of exposures	113
Measurement duration (h)	24
Absorption coefficient (mm^{-1})	26.379
$F(000)$	1772
θ range (deg.)	2.68–30.42
Range in $h\,k\,l$	$\pm 12, -15/+13, \pm 15$
Total no. reflections	10704
Independent reflections	2899 ($R_{int} = 0.0633$)
Reflections with $I > 2\sigma(I)$	2053 ($R_\sigma = 0.0591$)
Data/parameters	2899/215
Absorption correction	Numerical (HABITUS [47])
Transm. ratio (min/max)	0.4444/0.6581
Goodness-of-fit (F^2)	0.889
Final R indices ($I > 2\sigma(I)$)	$R_1 = 0.0401$
	$wR_2 = 0.0913$
R indices (all data)	$R_1 = 0.0584$
	$wR_2 = 0.0967$
Extinction coefficient	0.0006(2)
Larg. diff. peak and hole ($eÅ^{-3}$)	2.3/−2.2

systematic extinctions $h\,0\,l$ with $h + l \neq 2n$, $0\,k\,0$ with $k \neq 2n$, $h\,0\,0$ with $h \neq 2n$, and $0\,0\,l$ with $l \neq 2n$, the space group $P2_1/n$ (No. 14) was derived. The starting positional parameters were deduced from an automatic interpretation of direct methods with SHELXS-97 [48]. The structure of $Ce_6(BO_4)_2Ge_9O_{22}$ was refined with anisotropic displacement parameters for all atoms with SHELXL-97 [49] (full-matrix least-squares on F^2). The final difference Fourier synthesis did not reveal any significant residual peaks in the refinement (see Table 1). Details of the single-crystal structure measurement are shown in Table 1. Additionally, the positional parameters (Table 2), anisotropic displacement parameters (Table 3), and interatomic distances (Table 4) are listed. Further details of the crystal structure investigation may be obtained from the Fachinformationszentrum Karlsruhe, 76344 Eggenstein Leopoldshafen, Germany (fax: +49 7247 808 666; e-mail: crysdata@fiz-karlsruhe.de), on quoting the depository number CSD-391342.

Table 2
Atomic coordinates and isotropic equivalent displacement parameters U_{eq} ($Å^2$) for $Ce_6(BO_4)_2Ge_9O_{22}$ (space group: $P2_1/n$)

Atom	Wyckoff site	x	y	z	U_{eq}
Ce1	4*e*	0.04490(6)	0.66854(5)	0.05792(5)	0.0084(2)
Ce2	4*e*	0.65196(6)	0.83259(5)	0.94610(5)	0.0093(2)
Ce3	4*e*	0.99656(6)	0.82240(5)	0.73165(5)	0.0077(2)
B1	4*e*	0.779(2)	0.663(2)	0.475(2)	0.010(2)
Ge1	4*e*	0.8644(2)	0.8279(1)	0.2372(1)	0.0076(2)
Ge2	4*e*	0.7492(2)	0.5822(1)	0.7511(1)	0.0073(2)
Ge3	2*a*	0	0	0	0.0077(3)
Ge4	4*e*	0.8751(2)	0.5146(1)	0.2603(1)	0.0073(2)
Ge5	4*e*	0.3452(2)	0.5381(1)	0.9685(1)	0.0080(2)
O1	4*e*	0.8543(8)	0.6864(6)	0.8639(7)	0.011(2)
O2	4*e*	0.1387(7)	0.0258(6)	0.1386(6)	0.007(2)
O3	4*e*	0.1333(8)	0.5174(7)	0.9171(6)	0.009(2)
O4	4*e*	0.8263(8)	0.6707(6)	0.1958(7)	0.010(2)
O5	4*e*	0.2972(8)	0.5466(6)	0.1280(7)	0.011(2)
O6	4*e*	0.0763(8)	0.8061(6)	0.2657(6)	0.009(2)
O7	4*e*	0.8560(8)	0.3567(6)	0.3130(7)	0.009(2)
O8	4*e*	0.8037(8)	0.6843(6)	0.6118(6)	0.009(2)
O9	4*e*	0.8556(8)	0.9849(6)	0.2908(7)	0.010(2)
O10	4*e*	0.0808(7)	0.5314(6)	0.2666(7)	0.008(2)
O11	4*e*	0.1169(8)	0.8660(6)	0.9395(7)	0.010(2)
O12	4*e*	0.1090(8)	0.1292(7)	0.9284(7)	0.011(2)
O13	4*e*	0.4499(8)	0.3910(6)	0.9853(7)	0.011(2)
O14	4*e*	0.8789(8)	0.5686(6)	0.4284(7)	0.008(2)
O15	4*e*	0.3109(9)	0.7110(7)	0.9140(7)	0.012(2)

U_{eq} is defined as one third of the trace of the orthogonalized U_{ij} tensor.

Table 3
Anisotropic displacement parameters ($Å^2$) for $Ce_6(BO_4)_2Ge_9O_{22}$ (space group: $P2_1/n$).

Atom	U_{11}	U_{22}	U_{33}	U_{23}	U_{13}	U_{12}
Ce1	0.0091(2)	0.0075(2)	0.0088(3)	0.0000(2)	0.0023(2)	0.0006(2)
Ce2	0.0083(2)	0.0109(3)	0.0086(3)	0.0006(2)	0.0008(2)	−0.0001(2)
Ce3	0.0084(2)	0.0066(2)	0.0082(3)	−0.0001(2)	0.0015(2)	−0.0002(2)
B1	0.004(4)	0.017(5)	0.009(5)	−0.002(4)	0.003(4)	−0.002(4)
Ge1	0.0082(4)	0.0055(4)	0.0092(5)	−0.0008(4)	0.0016(4)	−0.0003(4)
Ge2	0.0078(4)	0.0064(4)	0.0078(5)	−0.0004(3)	0.0009(4)	0.0000(3)
Ge3	0.0088(6)	0.0060(6)	0.0085(7)	−0.0009(5)	0.0018(6)	−0.0002(5)
Ge4	0.0075(4)	0.0061(4)	0.0084(5)	−0.0001(3)	0.0012(4)	−0.0001(3)
Ge5	0.0083(5)	0.0085(5)	0.0072(5)	0.0001(4)	0.0009(4)	0.0004(4)
O1	0.009(3)	0.009(3)	0.013(4)	−0.002(3)	−0.002(3)	0.002(2)
O2	0.004(3)	0.009(3)	0.010(3)	0.005(2)	0.003(3)	0.004(2)
O3	0.007(3)	0.014(3)	0.007(3)	0.001(3)	0.002(3)	−0.002(3)
O4	0.0012(3)	0.004(3)	0.014(3)	0.002(3)	−0.003(3)	−0.001(2)
O5	0.014(3)	0.008(3)	0.010(3)	0.004(3)	0.004(3)	0.000(3)
O6	0.007(3)	0.011(3)	0.007(3)	0.001(2)	0.001(3)	0.001(2)
O7	0.009(3)	0.009(3)	0.010(3)	0.001(3)	0.002(3)	−0.002(2)
O8	0.013(3)	0.008(3)	0.007(3)	0.007(2)	0.001(3)	0.000(3)
O9	0.011(3)	0.008(3)	0.012(4)	−0.005(3)	0.002(3)	0.001(3)
O10	0.004(3)	0.005(3)	0.017(4)	0.002(2)	0.002(3)	−0.003(2)
O11	0.008(3)	0.010(3)	0.011(3)	0.000(3)	−0.002(3)	0.000(2)
O12	0.013(3)	0.009(3)	0.011(3)	0.001(3)	0.006(3)	0.002(3)
O13	0.018(4)	0.010(3)	0.006(3)	−0.002(2)	0.008(3)	−0.001(3)
O14	0.005(3)	0.007(3)	0.011(4)	0.001(2)	0.000(3)	0.002(2)
O15	0.019(4)	0.007(3)	0.009(3)	0.006(3)	−0.002(3)	0.004(3)

Table 4
Interatomic distances (pm) calculated with the single crystal lattice parameters in $Ce_6(BO_4)_2Ge_9O_{22}$

Ce1–O3a	241.1(7)	Ce2–O12	241.1(8)	Ce3–O7	240.2(7)	Ge1–O4	177.8(7)
Ce1–O4	254.6(7)	Ce2–O10	245.9(7)	Ce3–O11	242.4(7)	Ge1–O9	179.5(7)
Ce1–O1	254.8(8)	Ce2–O6	249.1(7)	Ce3–O5	243.0(8)	Ge1–O6	186.7(7)
Ce1–O3b	257.5(7)	Ce2–O1	259.9(7)	Ce3–O1	247.3(7)	Ge1–O12	188.4(7)
Ce1–O12	257.9(7)	Ce2–O14	261.0(7)	Ce3–O9	247.6(7)	Ge1–O7	197.8(7)
Ce1–O11	259.6(7)	Ce2–O7	262.0(7)	Ce3–O8	251.0(7)	Ge1–O15	205.5(7)
Ce1–O5	261.8(7)	Ce2–O2	262.5(6)	Ce3–O2	252.9(6)		
Ce1–O6	268.0(7)	Ce2–O13	270.3(7)	Ce3–O13	254.5(7)		∅189.3
Ce1–O10	268.6(7)	Ce2–O14	291.1(7)	Ce3–O4	295.8(7)		
Ce1–O8	278.3(7)					B1–O11	147(2)
Ce1–O15	296.9(7)					B1–O8	149(2)
	∅263.6		∅260.3		∅252.7	B1–O15	155(2)
						B1–O14	146(2)
							∅149
Ge2–O1	183.4(7)	Ge3–O2a	184.9(7)	Ge4–O10	180.8(6)	Ge5–O5	181.6(7)
Ge2–O2	187.8(7)	Ge3–O2b	184.9(7)	Ge4–O7	181.0(7)	Ge5–O13a	183.4(7)
Ge2–O10	195.4(7)	Ge3–O12a	189.9(7)	Ge4–O4	185.6(7)	Ge5–O3	189.8(7)
Ge2–O6	195.7(7)	Ge3–O12b	189.9(7)	Ge4–O14	190.3(7)	Ge5–O9	194.5(7)
Ge2–O8	196.2(6)	Ge3–O11a	192.5(7)	Ge4–O3	193.9(7)	Ge5–O13b	196.9(8)
Ge2–O5	197.7(7)	Ge3–O11b	192.5(7)	Ge4–O9	206.6(7)	Ge5–O15	197.1(7)
	∅192.7		∅189.1		∅189.7		∅190.6

Standard deviations in parentheses.

4. Results and discussion

The crystal structure of the new borogermanate $Ce_6(BO_4)_2Ge_9O_{22}$ is built up from corner- and edge-sharing GeO_6-octahedra, which are furthermore connected via corner-sharing BO_4-tetrahedra. Fig. 1 gives a view of the structure of $Ce_6(BO_4)_2Ge_9O_{22}$, where the GeO_6-octahedra and BO_4-tetrahedra are represented as light and dark polyhedra, respectively. The remaining voids inside the polyhedral arrangement are filled with cerium ions. Fig. 2 offers a more detailed view of the linkage between octahedra and tetrahedra in the *ac*-plane. In detail, six octahedra are edge-linked to form a Ge_6O_{24}-group, and three octahedra are connected via common corners to generate a Ge_3O_{16}-group. These groups are connected among each other and additionally interconnected by BO_4-tetrahedra to result in a network structure from GeO_6-octahedra and BO_4-tetrahedra. Fig. 3 shows the coordination of the three crystallographically distinguishable cerium ions. They are coordinated by 11 (Ce1) and 9 (Ce2 and Ce3) oxygen atoms in a distance of 240–297 pm. These values correspond to the distance range in the recently published high-pressure *meta*-borate γ-$Ce(BO_2)_3$, where the cerium cations are coordinated by 10 oxygen atoms in a distance between 239 and 303 pm with an average value of 265.8 pm [5]. Due to the pressure-coordination rule [50], the high-pressure phases $Ce_6(BO_4)_2Ge_9O_{22}$ and γ-$Ce(BO_2)_3$ possess high coordination numbers and large Ce–O distances in contrast to known cerium borates like α-$Ce(BO_2)_3$ [51] (C.N.: 10) with Ce–O distances of 236–276 pm, λ-$CeBO_3$ [51] (C.N.: 9) with 239–272 pm, H-$CeBO_3$ [51] (C.N.: 9) with 244–275 pm, and an oxide like

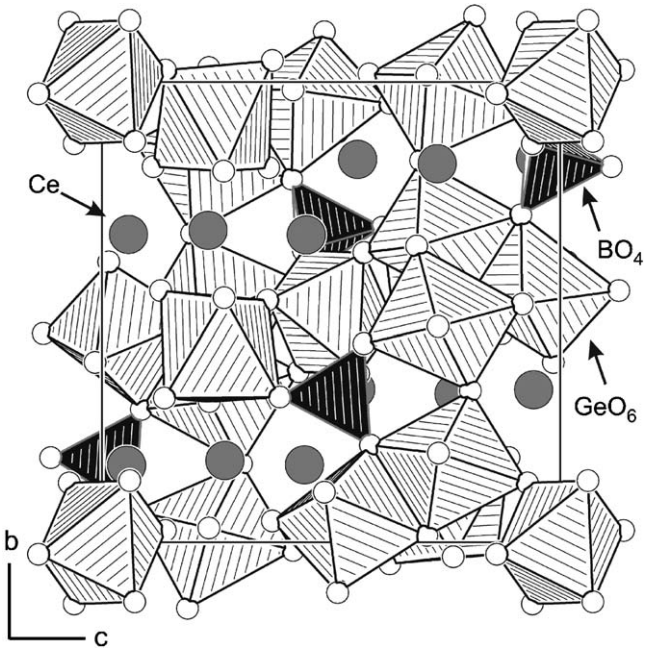

Fig. 1. Crystal structure of $Ce_6(BO_4)_2Ge_9O_{22}$, view along [1 0 0]. The cerium cations are shown as large grey spheres and the oxygen atoms as white spheres. The GeO_6-octahedra and BO_4-tetrahedra are given in the polyhedral representation.

Ce_2O_3 [52] (C.N.: 7) with 234–269 pm. A closer view of the coordination sphere of Ce1 in $Ce_6(BO_4)_2Ge_9O_{22}$ shows a gap between the 10 nearest oxygen atoms ranging from 241–279 pm and the 11th oxygen atom in a distance of 297 pm. Nevertheless, Madelung part of lattice energy (MAPLE) calculations [53–55] confirmed the coordinative

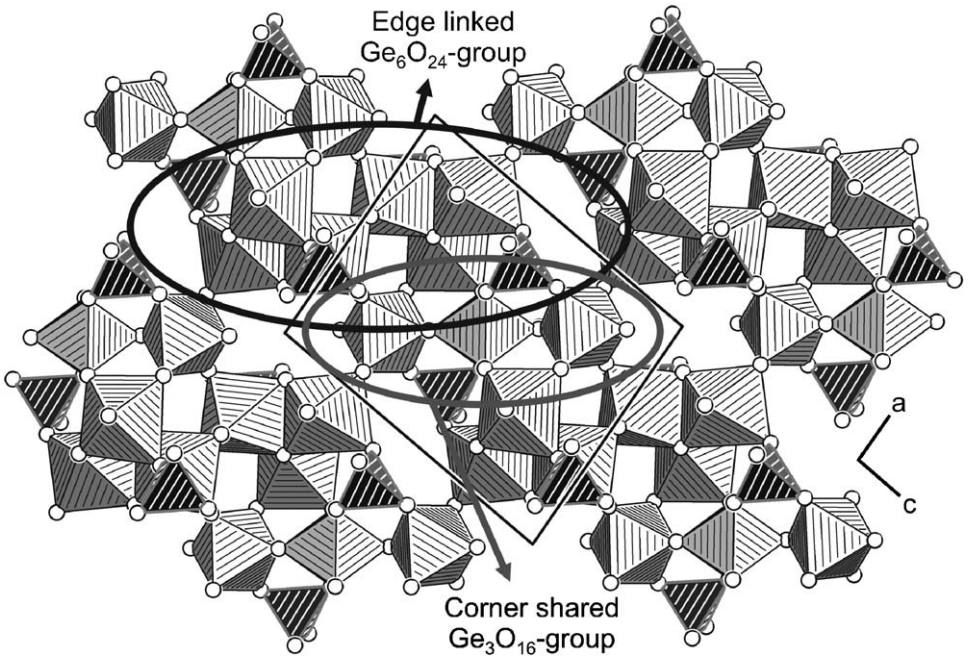

Fig. 2. Crystal structure of $Ce_6(BO_4)_2Ge_9O_{22}$, view along [010].

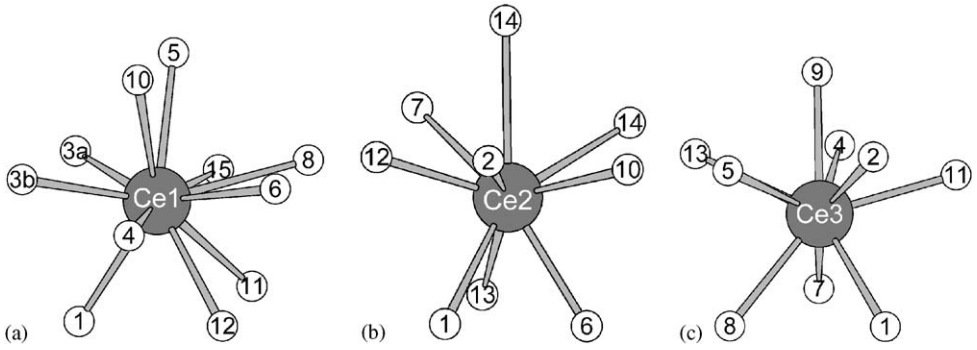

Fig. 3. Coordination spheres of the Ce^{3+} ions in the crystal structure of $Ce_6(BO_4)_2Ge_9O_{22}$.

contribution of this oxygen atom followed by the next oxygen atom in a distance of 400 pm, without any coordinative contribution. In the case of Ce3, the gap is much more pronounced (between 255 and 296 pm), but the coordinative contribution of this oxygen is also confirmed by the MAPLE calculations.

In the tetrahedral BO_4-group, the B–O distances vary between 147 and 155 pm. With the exception of the largest value (155 pm), the B–O distances correspond well with the known average value of 147.6 pm for borates [56,57]. Fig. 4 gives a view of the coordination sphere of O15, featuring the large distance of 155 pm to the boron atom. In fact, O15 is a three-coordinated oxygen atom $O^{[3]}$, possessing a significantly longer distance to boron than two-fold coordinated oxygen atoms. Three coordinated oxygen atoms can be found in a few minerals like *tunnelite* ($SrB_6O_9(OH)_2 \cdot 3H_2O$) [58], *strontioginorite* ($(Sr,Ca)_2B_{14}O_{20}(OH)_6 \cdot 5H_2O$) [59], *aristarainite* ($Na_2Mg[B_6O_8(OH)_4]_2 \cdot 4H_2O$) [60], and synthetic borates like SrB_4O_7 [61–63], PbB_4O_7 [62,64], and EuB_4O_7 [65]. More often, $O^{[3]}$ was observed in high-pressure phases like β-ZnB_4O_7 [66], β-CaB_4O_7 [67], β-HgB_4O_7 [68], β-$RE(BO_2)_3$ [2,3], γ-$RE(BO_2)_3$ [4,5], and the high-pressure modification of B_2O_3 [69] itself. The corresponding average $B–O^{[3]}$ distances in these compounds range around 155 pm.

The O–B–O angles inside of the BO_4-tetrahedra range from 105° to 115° with an average value of 109.4°. The two B–O–Ge angles and the Ge–O–Ge one at $O^{[3]}$ are 137.2(6)°, 129.9(6)°, and 92.3(3)°, respectively (see Fig. 4). As far as we know, $Ce_6(BO_4)_2Ge_9O_{22}$ is the first structure, in which a three-fold coordinated oxygen atom, bonded to one boron and two germanium atoms, was observed.

The Ge–O distances inside the GeO_6 octahedra range from 178–207 pm with an average value of 190.3 pm, which corresponds well with known average values of Ge–O distances in GeO_6-octahedra, e.g. 189.9 pm in $La_2Ge_3O_9$

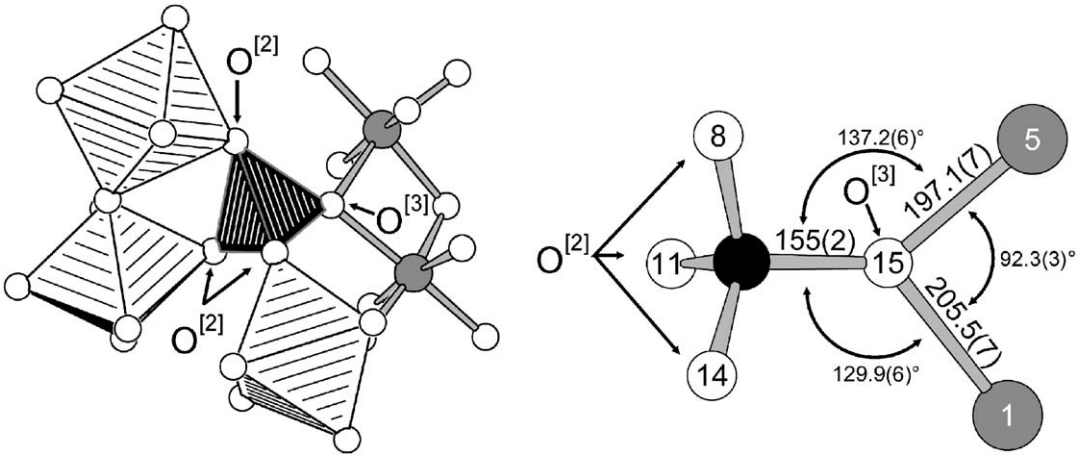

Fig. 4. Environment of the three-fold coordinated oxygen atom in $Ce_6(BO_4)_2Ge_9O_{22}$. Left: representation of the polyhedral environment of the three-fold coordinated oxygen $O^{[3]}$. Right: distances and angles around oxygen fifteen ($O^{[3]}$). (Boron: black sphere; germanium: grey sphere; oxygen: light sphere.)

Table 5
Charge distribution in $Ce_6(BO_4)_2Ge_9O_{22}$, calculated with the bond-length/bond-strength concept (ΣV) [72,73] and the CHARDI concept (ΣQ) [74]

	Ce1	Ce2	Ce3	Ge1	Ge2	Ge3	Ge4	Ge5
ΣQ	+2.99	+2.96	+2.95	+3.96	+3.97	+3.74	+3.89	+4.17
ΣV	+3.11	+2.53	+3.11	+4.20	+3.74	+4.09	+4.12	+3.98
	O1	O2	O3	O4	O5	O6	O7	O8
ΣQ	−1.90	−2.16	−1.98	−2.07	−2.11	−1.98	−2.07	−1.86
ΣV	−1.76	−2.05	−2.00	−2.09	−2.06	−1.88	−2.10	−1.80
	O9	O10	O11	O12	O13	O14	O15	B1
ΣQ	−2.15	−2.16	−2.13	−2.13	−1.90	−1.91	−1.49	+3.24
ΣV	−2.27	−2.03	−2.10	−2.09	−1.86	−1.82	−1.77	+2.89

[70], 189.4 pm in $Ce_2Ge_3O_9$ [70], 188.5 pm in rutile-type GeO_2 [71], and 199.7 pm in $Ni_5GeB_2O_{10}$ [41].

For better evidence, we calculated bond-valence sums for $Ce_6(BO_4)_2Ge_9O_{22}$ with the bond-length/bond-strength [72,73] and charge distribution in solids (CHARDI) concept (Table 5) [74]. The formal ionic charges of the atoms, acquired by the X-ray structure analysis, are in agreement within the limits of the concepts, except oxygen fifteen, which shows values of −1.77 (ΣV) and −1.49 (ΣQ). As shown in Fig. 4, this oxygen atom (O15) is coordinated to one boron and two germanium atoms with relatively high distances. This situation leads to lower values than expected and can be compared to calculated values of three-coordinated oxygen atoms $O^{[3]}$ in former mentioned borates like β-ZnB_4O_7 [66] ($O^{[3]}$: −1.83 (ΣV); −1.67 (ΣQ)), β-CaB_4O_7 [67] ($O^{[3]}$: −1.77 (ΣV); −1.92 (ΣQ)), β-HgB_4O_7 [68] ($O^{[3]}$: −2.06 (ΣV); −1.83 (ΣQ)), β-$Er(BO_2)_3$ [2] ($O^{[3]}$: −1.96 (ΣV); −1.76(ΣQ)), and γ-$Ce(BO_2)_3$ [5] ($O^{[3]}$: −1.91 (ΣV); −1.62(ΣQ)). These examples represent $O^{[3]}$ atoms exclusively coordinated by boron, whereas the $O^{[3]}$ atoms in $Ce_6(BO_4)_2Ge_9O_{22}$ are linked to one boron and two germanium atoms. Due to the higher distances between germanium and oxygen (197.1(7) and 205.5(7) pm), compared to the distance between boron and oxygen (155(2) pm), the deviation from the expected value −2 is larger than in the corresponding borates.

Additionally, we calculated the MAPLE value [53–55] for $Ce_6(BO_4)_2Ge_9O_{22}$ to compare it with the MAPLE value from the binary components Ce_2O_3, GeO_2, and the high-pressure modification B_2O_3-II [$3Ce_2O_3$ (14150 kJ mol^{-1}) [75] + $9GeO_2$ (*rutile* type; *argutite*) (14207 kJ mol^{-1}) [76] + $1B_2O_3$-II (21938 kJ mol^{-1})] [69]. The deviation of the calculated value of 191881 kJ mol^{-1} for $Ce_6(BO_4)_2Ge_9O_{22}$ differs only 0.2% compared with the MAPLE value obtained from the binary oxides (192251 kJ mol^{-1}).

4.1. Thermal behaviour of $Ce_6(BO_4)_2Ge_9O_{22}$

Temperature-dependent X-ray powder diffraction experiments were performed on a STOE Stadi P powder diffractometer (Mo-$K\alpha$) with a computer-controlled STOE furnace: The sample was enclosed in a quartz capillary and heated from room temperature to 500 °C in steps of 100 °C, from 500 to 1100 °C in steps of 50 °C, and back to 550 °C in steps of 50 °C. At each temperature, a diffraction pattern was recorded over the angular range $4° \leqslant 2\theta \leqslant 20°$. In the

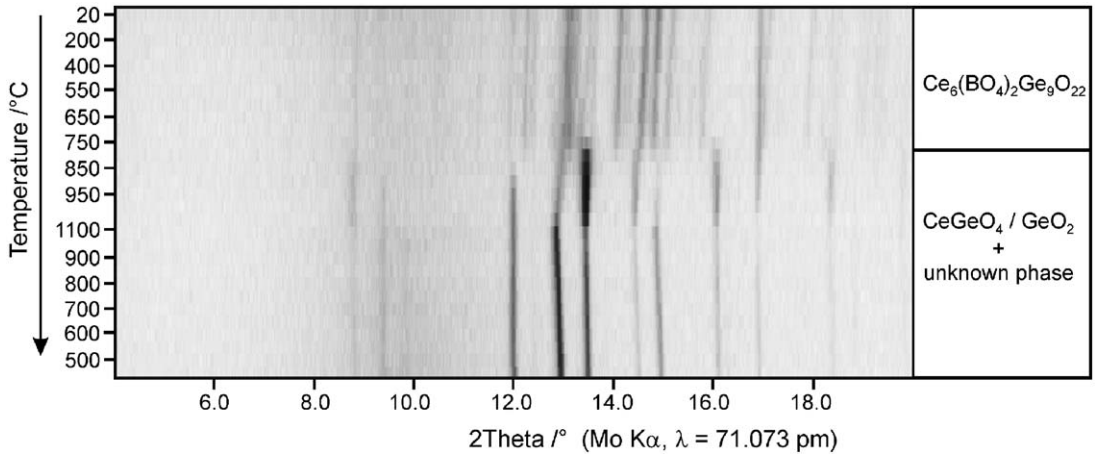

Fig. 5. Temperature-dependent X-ray powder patterns, following the decomposition reaction of the metastable high-pressure phase $Ce_6(BO_4)_2Ge_9O_{22}$.

temperature range 500 °C to room temperature, no diffraction data were received due to a mark capillary breakage. Fig. 5 gives a view of the powder patterns, in which the reflections of the borogermanate $Ce_6(BO_4)_2Ge_9O_{22}$ can be detected up to a temperature of 750 °C. Further heating (750–1000 °C) led to a decomposition of $Ce_6(BO_4)_2Ge_9O_{22}$ into the rare-earth germanate $CeGeO_4$ [77], GeO_2 (*argutite*), B_2O_3 in its probably molten state, and a phase, which is still unknown. Subsequent cooling to 550 °C showed that all three phases endured. The reflections near 9° and 17° are artefacts from the furnace. From these results, we presume that the high-pressure phase $Ce_6(BO_4)_2Ge_9O_{22}$ has a metastable character under ambient pressure conditions.

5. Conclusions

In this paper, we described the synthesis of the new borogermanate $Ce_6(BO_4)_2Ge_9O_{22}$ via multianvil high-pressure techniques from CeO_2, GeO_2, and B_2O_3. The structure was solved from single-crystal data. Following the pressure-coordination rule [50], the coordination numbers of boron and germanium exhibit the highest known values 4 and 6, respectively. In contrast to all known borogermanates, we were able to realize the simultaneous presence of BO_4-tetrahedra in combination with GeO_6-octahedra inside the structure of $Ce_6(BO_4)_2Ge_9O_{22}$ by use of high pressure. Additionally, a three-fold coordinated oxygen atom $O^{[3]}$, linked to one boron and two germanium atoms, was observed for the first time. From these results, we think it possible to have access to new high-pressure phases with interesting structural features in the substance class of borogermanates.

Acknowledgments

We gratefully acknowledge the continuous support of these investigations by Prof. Dr. W. Schnick, Department Chemie und Biochemie of the Ludwig-Maximilians-Universität München (Germany). Special thanks go to Dr. O. Oeckler and T. Miller (LMU München) for collecting the single-crystal data and to Dipl. Chem. S. Correll for the in-situ powder diffraction measurements. This work was financially supported by the Deutsche Forschungsgemeinschaft.

Reference

[1] H. Huppertz, B. von der Eltz, R.-D. Hoffmann, H. Piotrowski, J. Solid State Chem. 166 (2002) 203.
[2] H. Emme, T. Nikelski, Th. Schleid, R. Pöttgen, M.H. Möller, H. Huppertz, Z. Naturforsch, B: Chem. Sci. 59 (2004) 202.
[3] T. Nikelski, Th. Schleid, Z. Anorg. Allg. Chem. 629 (2003) 1017.
[4] H. Emme, C. Despotopoulou, H. Huppertz, Z. Anorg. Allg. Chem. 630 (2004) 1717.
[5] H. Emme, C. Despotopoulou, H. Huppertz, Z. Anorg. Allg. Chem. 630 (2004) 2450.
[6] H. Huppertz, B. von der Eltz, J. Am. Chem. Soc. 124 (2002) 9376.
[7] H. Huppertz, Z. Naturforsch, B: Chem. Sci. 58 (2003) 278.
[8] H. Huppertz, H. Emme, J. Phys.: Condens. Matter 16 (2004) S1283.
[9] H. Emme, H. Huppertz, Z. Anorg. Allg. Chem. 628 (2002) 2165.
[10] H. Emme, H. Huppertz, Chem. Eur. J. 9 (2003) 3623.
[11] H. Emme, H. Huppertz, Acta Crystallogr., Sect. C: Struct. Commun 61 (2005) i29.
[12] H. Emme, M. Valldor, R. Pöttgen, H. Huppertz, Chem. Mater. 17 (2005) 2707.
[13] B.F. Dzhurinskii, G.V. Lysanova, M.G. Komova, V.I. Chistova, E.G. Tselebrovskaya, Russ. J. Inorg. Chem. 36 (1991) 1991.
[14] G.V. Lysanova, B.F. Dzhurinskii, M.G. Komova, O.V. Sorokina, B.I. Chistova, Inorg. Mater. 24 (1988) 190.
[15] B.F. Dzhurinskii, A.B. Pobedina, K.K. Palkina, M.G. Komova, Russ. J. Inorg. Chem. 43 (1998) 1488.
[16] A.B. Ilyukhin, B.F. Dzhurinskii, Russ. J. Inorg. Chem. 39 (1994) 530.
[17] B.F. Dzhurinskii, G.V. Lysanova, M.G. Komova, L.Z. Gokhman, V.A. Krut′ko, Russ. J. Inorg. Chem. 40 (1995) 1699.
[18] B.F. Dzhurinskii, A.B. Ilyukhin, Russ. J. Inorg. Chem. 45 (2000) 1.
[19] G.A. Bandurkin, G.V. Lysanova, K.K. Palkina, V.A. Krut′ko, M.G. Komova, Russ. J. Inorg. Chem. 49 (2004) 213.
[20] K.K. Palkina, N.E. Kuz′mina, B.F. Dzhurinskii, A.B. Pobedina, V.P. Sanygin, A.M. Kvardakov, Russ. J. Inorg. Chem. 46 (2001) 465.
[21] A.B. Pobedina, M.G. Komova, B.F. Dzhurinskii, Russ. J. Inorg. Chem. 45 (2000) 1024.
[22] K.K. Palkina, N.E. Kuz′mina, B.F. Dzhurinskii, A.B. Pobedina, V.P. Sanygin, A.M. Kvardakov, Russ. J. Inorg. Chem. 44 (1999) 1817.

[23] K.K. Palkina, N.E. Kuz′mina, A.B. Pobedina, V.P. Sanygin, A.M. Kvardakov, B.F. Dzhurinskii, Russ. J. Inorg. Chem. 45 (2000) 1637.
[24] A.A. Kaminskii, B.V. Mill, E.L. Belokoneva, A.V. Butashin, Izv. Akad. Nauk SSSR, Neorg. Mater. 26 (1990) 1105.
[25] E. Antic-Fidancev, M. Lemaitre-Blaise, M. Taibi, J. Aride, A. Boukhari, P. Porcher, J. Alloys Compd. 275–277 (1998) 424.
[26] E.L. Belonkoneva, B.V. Mill, A.V. Butashin, A.A. Kaminskii, Izv. Akad. Nauk SSSR, Neorg. Mater. 27 (1991) 1700.
[27] G.V. Lysanova, B.F. Dzhurinskii, M.G. Komova, V.I. Tsaryuk, I.V. Tananaev, Inorg. Mater. 25 (1989) 545.
[28] M. Taibi, J. Airde, A. Boukhari, Ann. Chim. Sci. Mater. 23 (1998) 285.
[29] A. Rulmont, P. Tarte, J. Solid State Chem. 75 (1988) 244.
[30] A.A. Voronkov, Y.A. Pyantenko, Sov. Phys. Crystallogr. Engl. Trans. 12 (1967) 214.
[31] I.Y. Nekrasov, R.A. Nekrasov, Dokl. Akad. Nauk SSSR 201 (1970) 179.
[32] J. McAdrew, T.R. Scott, Nature 4480 (1955) 509.
[33] A. Gallegari, G. Giuseppeti, F. Mazzi, C. Tadini, Neues Jahrb. Miner., Monatsh. H2 (1992) 49.
[34] F.F. Foit, M.W. Phillips, G.V. Gibbs, Am. Mineral. 58 (1973) 909.
[35] M.S. Dadachov, K. Sun, T. Conradsson, X. Zou, Angew. Chem. 112 (2000) 3820;
M.S. Dadachov, K. Sun, T. Conradsson, X. Zou, Angew. Chem. Int. Ed. Engl. 39 (2000) 3674.
[36] Y. Li, X. Zou, Angew. Chem. 117 (2005) 2048;
Y. Li, X. Zou, Angew. Chem. Int. Ed. Engl. 44 (2005) 2012.
[37] Z.-E. Lin, J. Zhang, G.-Y. Yang, Inorg. Chem. 42 (2003) 1797.
[38] G.-M. Wang, Y.-Q. Sun, G.-Y. Yang, Cryst. Growth Des. 5 (2005) 313.
[39] H.-X. Zhang, J. Zhang, S.-T. Zheng, G.-M. Wang, G.-Y. Yang, Inorg. Chem. 43 (2004) 6148.
[40] H.-X. Zhang, J. Zhang, S.-T. Zheng, G.-Y. Yang, Inorg. Chem. 44 (2005) 1166.
[41] K. Bluhm, Hk. Müller-Buschbaum, J. Less-Common Met. 147 (1989) 133.
[42] O. Jarchow, K.H. Klaska, M. Ruks, B. Holtz, Z. Kristallogr. 211 (1996) 4.
[43] H. Huppertz, Z. Kristallogr. 219 (2004) 330.
[44] D. Walker, M.A. Carpenter, C.M. Hitch, Am. Mineral. 75 (1990) 1020.
[45] D. Walker, Am. Mineral. 76 (1991) 1092.
[46] D.C. Rubie, Phase Trans. 68 (1999) 431.
[47] W. Herrendorf, H. Bärnighausen, HABITUS—Program for Numerical Absorption Correction, University of Karlsruhe/Giessen, Germany, 1993/1997.
[48] G.M. Sheldrick, SHELXS-97, Program for the Solution of Crystal Structures, University of Göttingen, Germany, 1997.
[49] G.M. Sheldrick, SHELXL-97, Program for Crystal Structure Refinement, University of Göttingen, Germany, 1997.
[50] A. Neuhaus, Chimia 18 (1964) 93.
[51] F. Goubin, Y. Montardi, P. Deniard, X. Rocquefelte, R. Brec, S. Jobic, J. Solid State Chem. 177 (2004) 89.
[52] H. Bärnighausen, G. Schiller, J. Less-Common Met. 110 (1985) 185.
[53] R. Hoppe, Angew. Chem. 78 (1966) 52;
R. Hoppe, Angew. Chem. Int. Ed. Engl. 5 (1966) 95.
[54] R. Hoppe, Angew. Chem. 82 (1970) 7;
R. Hoppe, Angew. Chem. Int. Ed. Engl. 9 (1970) 25.
[55] R. Hübenthal, MAPLE, Program for the Calculation of MAPLE Values, Vers. 4, University of Giessen, Germany, 1993.
[56] E. Zobetz, Z. Kristallogr. 191 (1990) 45.
[57] F.C. Hawthorne, P.C. Burns, J.D. Grice, Rev. Mineral. 33 (1996) 42.
[58] J.R. Clark, Am. Mineral. 49 (1964) 1549.
[59] J.A. Konnert, J.R. Clark, C.L. Christ, Am. Mineral. 55 (1970) 1911.
[60] S. Ghose, C. Wan, Am. Mineral. 62 (1977) 979.
[61] J. Krogh-Moe, Acta Chem. Scand. 18 (1964) 2055.
[62] A. Perloff, S. Block, Acta Crystallogr. 20 (1966) 274.
[63] F. Pan, G. Shen, R. Wang, X. Wang, D. Shen, J. Cryst. Growth 241 (2002) 108.
[64] D.L. Corker, A.M. Glazer, Acta Crystallogr. Sect. B 52 (1996) 260.
[65] K.-I. Machida, G.-Y. Adachi, J. Shiokawa, Acta Crystallogr. Sect. B 36 (1980) 2008.
[66] H. Huppertz, G. Heymann, Solid State Sci. 5 (2003) 281.
[67] H. Huppertz, Z. Naturforsch, B: Chem. Sci. 58b (2003) 257.
[68] H. Emme, M. Weil, H. Huppertz, Z. Naturforsch, B: Chem. Sci. 60 (2005) 815.
[69] C.T. Prewitt, R.D. Shannon, Acta Crystallogr. Sect. B 24 (1968) 869.
[70] O. Jarchow, K.H. Klaska, M. Ruks, B. Holtz, Z. Kristallogr. 211 (1996) 4.
[71] A.A. Bolzan, C. Fong, B.J. Kennedy, C.J. Howard, Acta Crystallogr. Sect. B 53 (1997) 373.
[72] I.D. Brown, D. Altermatt, Acta Crystallogr. Sect. B 41 (1985) 244.
[73] N.E. Brese, M. O'Keeffe, Acta Crystallogr. Sect. B 47 (1991) 192.
[74] R. Hoppe, S. Voigt, H. Glaum, J. Kissel, H.P. Müller, K. Bernet, J. Less-Common Met. 156 (1989) 105.
[75] K. Aurivillius, Acta Crystallogr. 9 (1956) 685.
[76] Z. Lodziana, K. Parlinski, J. Hafner, Phys. Rev. B 63 (2001) 134106.
[77] F. Bertaut, A. Durif, Compt. Rend. 238 (1954) 2173.